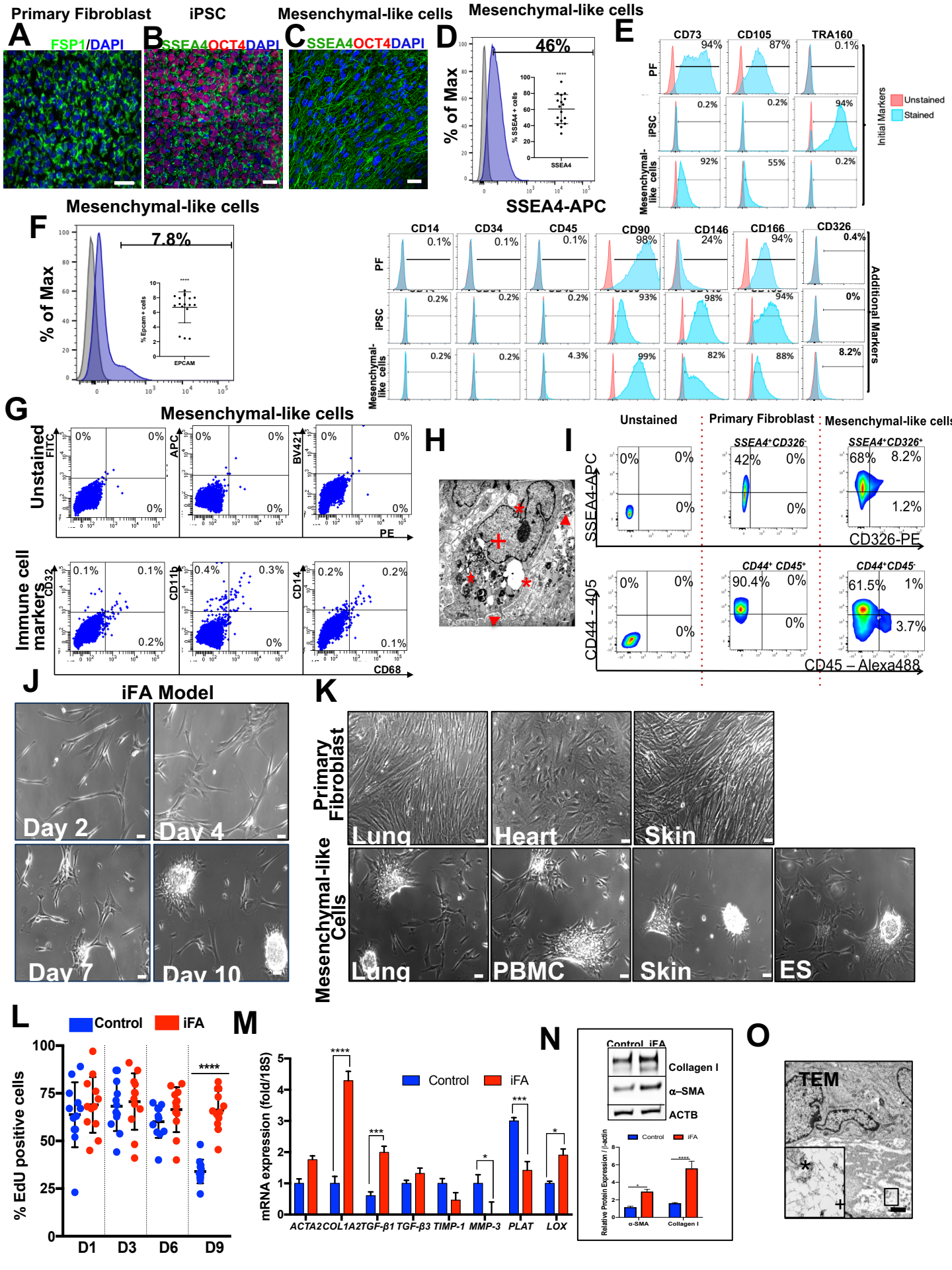


Cell Reports, Volume 29

Supplemental Information

Modeling Progressive Fibrosis with Pluripotent Stem Cells Identifies an Anti-fibrotic Small Molecule

Preethi Vijayaraj, Aspram Minasyan, Abdo Durra, Saravanan Karumbayaram, Mehrsa Mehrabi, Cody J. Aros, Sarah D. Ahadome, David W. Shia, Katherine Chung, Jenna M. Sandlin, Kelly F. Darmawan, Kush V. Bhatt, Chase C. Manze, Manash K. Paul, Dan C. Wilkinson, Weihong Yan, Amander T. Clark, Tammy M. Rickabaugh, W. Dean Wallace, Thomas G. Graeber, Robert Damoiseaux, and Brigitte N. Gomperts



1 **Figure S1. Generation and characterization of iPSC-derived mesenchymal-like cells. Related to**
2 **Figure 1**

3 (A-C) Steps involved in generation of mesenchymal-like cells. (A) Primary cultures of lung fibroblasts that
4 expressed the fibroblast marker FSP1. (B) The primary fibroblasts were reprogrammed into iPSC and
5 expressed pluripotency marker OCT4. (C) The iPSCs were differentiated into cells that expressed markers
6 largely mesenchymal-like cells (SSEA4+). (D) Overlaid histogram plot that depicts the relative SSEA4
7 fluorescence intensity (blue) of the mesenchymal-like cells compared to the unstained controls (grey). Inset
8 depicts % of positive cells (n=17). $p \leq 0.0001$ by Wilcoxon signed rank test. (E) Representative flow
9 cytometric analysis results before and after differentiation of iPSCs. Representative flow cytometric
10 profiles obtained from parent primary fibroblasts, undifferentiated iPSC and from mesenchymal stem cell
11 (MSC)-like cells obtained after successful differentiation of iPSC to mesenchymal-like cells. The red
12 histograms represent the isotype controls, while the blue histograms represent the individual markers being
13 analyzed. (F) Overlaid histogram plot that depicts the relative CD326 (epithelial marker) fluorescence
14 intensity (blue) of the mesenchymal-like cells compared to the unstained controls (grey). Inset depicts %
15 positive cells (n=17). $p \leq 0.0001$ by Wilcoxon signed rank test. (G) Representative FACS plots revealing
16 expression of monocyte/macrophage markers in the mesenchymal-like cells. The cells were co-stained for
17 CD68 and CD32, CD11b or CD14, revealing 0.2-0.7% cells positive for monocyte/macrophage markers.
18 Unstained controls are shown in top panel (n=7). $p = 0.0156$ by Wilcoxon signed rank test. (H)
19 Representative image of mesenchymal-like cell of a macrophage-like cell displaying heterochromatin (+),
20 vacuolated cytoplasm (*), several microvilli (arrows) and whorls of phagocytosed matter (star). Scale bar,
21 $1 \mu\text{m}$. (I) Characterization of primary fibroblasts (middle panel) and mesenchymal-like cells (right panel)
22 using multi-color FACS. Unstained control plots are shown on the left panel. Representative FACS data
23 with gating are shown for each marker. (J) Phase-contrast images demonstrating propagation of
24 mesenchymal-like cells on 13 kPa hydrogels (iFA) over time that reveal progressively increasing scar-like
25 aggregate size with progression from D2 to 10; Scale bar, $50 \mu\text{m}$. (K) Phase-contrast images demonstrating
26 the development of the iFA phenotype only in cultures from mesenchymal-like cells generated from iPSCs
27 of different sources and human ES cells. Primary fibroblasts failed to generate the phenotype irrespective
28 of the parent source. Scale bar, $50 \mu\text{m}$. (L) Quantification of EdU positive cells in primary fibroblasts and

29 mesenchymal-like cells grown on 13kPa hydrogels related to Figure 1B. All data are presented as mean \pm
30 s.e.m; **** $P < 0.0001$ using 2-way ANOVA followed by Tukey's multiple comparisons test. **(M)** Fibrosis-
31 related genes expression by qPCR in primary fibroblasts (control) and mesenchymal-like cells (iFA)
32 cultured on 13kPa hydrogels (n=5). **(N)** Representative immunoblot analysis of the expression of Collagen
33 I and α -SMA in primary fibroblasts (control) and mesenchymal-like cells (iFA) showing increased
34 expression of the fibrosis-related proteins in the iFA cultures collected at day 13 (left panel). Beta actin was
35 used as a loading control. Right panel shows quantitative data presented as mean \pm s.e.m; **** $P < 0.0001$,
36 * $P < 0.05$ using 2-way ANOVA followed by Sidak's multiple comparisons test. **(O)** Representative
37 transmission electron microscopic (TEM) images showing ultrastructure of cells in the iFA model amidst
38 copious amounts of matricellular proteins (asterisk) and fibrillar proteins (plus). Inset is a higher
39 magnification of the TEM image; Scale bar, 1 μ m.

40

41

42

43

44

45

46

47

48

49

50

51

52

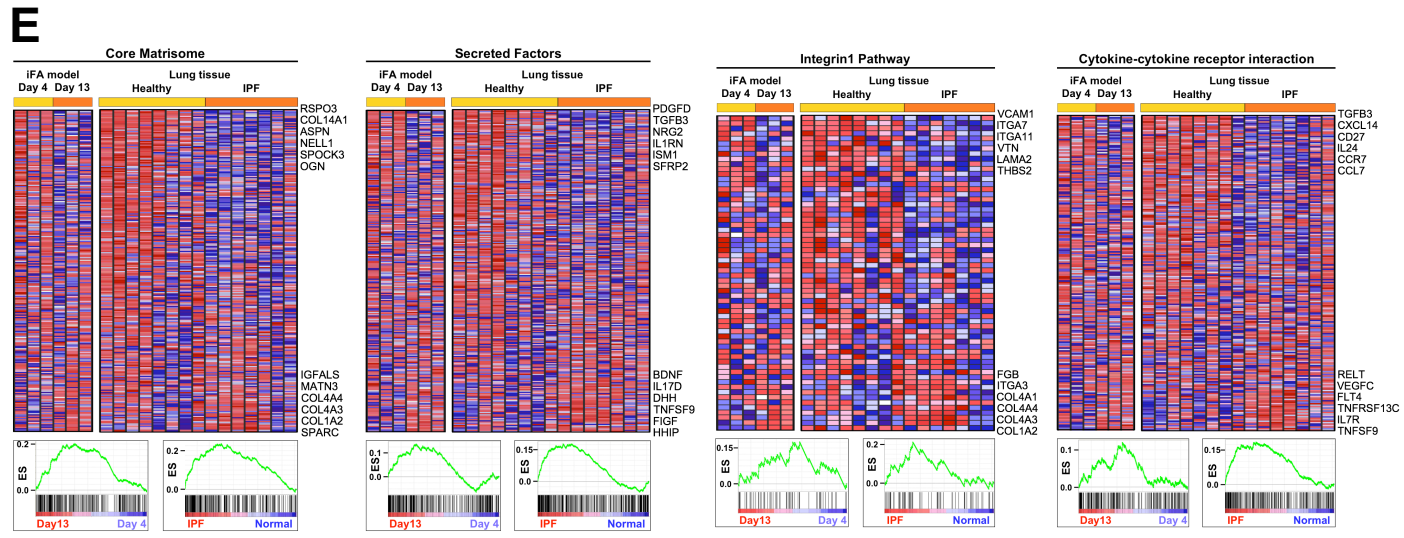
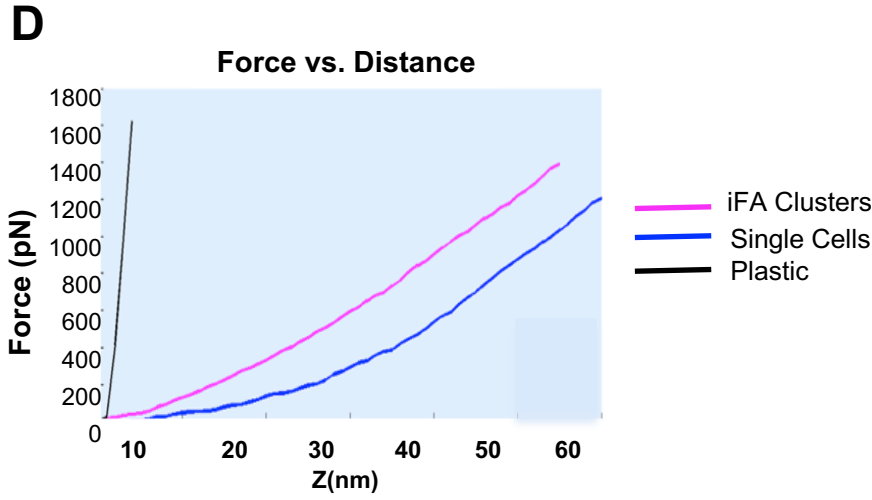
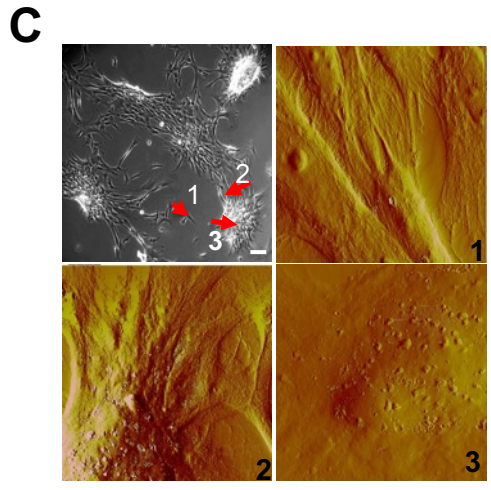
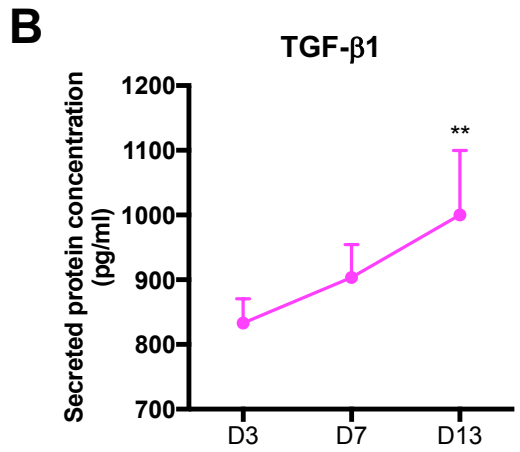
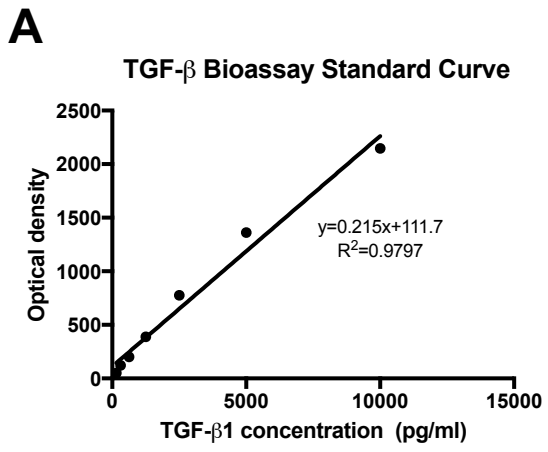
53

54

55

56

FIGURE S2



57 **Figure S2. Characterization of the iFA phenotype. Related to Figure 2**

58 (A) PAI-1 promoter/luciferase construct-transfected mink lung epithelial cells were incubated with various
59 concentrations of human recombinant(r) TGF- β 1 at 37°C for 20 h. The standard curve showed a dose-
60 dependent increase in luciferase activity (relative light units, RLU) by rTGF- β 1 between 0 and 10 ng/ml.
61 The standard curve was used to determine the bioactivity of TGF- β in the iFA model. (B) Time-dependent
62 levels of secreted TGF- β 1 during the development of the iFA phenotype (D4 to 13). A significant increase
63 in secreted TGF- β 1 protein in the iFA model was observed over time similar to that reported in fibrotic
64 organs (n=6). Data represent mean \pm s.e.m; ** P <0.01 using 2-way ANOVA and Sidak's multiple
65 comparisons test. (C) Representative phase contrast image (top left) of the iFA model at D13 that was used
66 to measure the elastic modulus. Arrows point to representative regions of the culture where the
67 measurements were made. 1 refers to single cells in the dish. 2 refers to the cells on the periphery of the
68 iFA phenotype. 3 refers to the center of the iFA phenotype. 3D rendering of the AFM amplitude channel
69 that shows representative areas of 1,2 and 3 from panel (top right and bottom panels). (D) Force versus
70 distance curves measured on cells from (c). Black line depicts the curve obtained on the stiff petri dish.
71 Magenta line represents curve obtained from cells in the iFA and blue line represents single cells. The
72 measured indentation was fitted to the Sneddon model. Elastic moduli of iFA cells and single cells were
73 calculated as 30kPa and 15kPa, respectively. (E) Heatmaps showing expression of genes (red/blue are
74 up/down-regulated), encoding for selected canonical pathways (core matrisome, selected factors, integrin 1
75 and cytokine-cytokine receptor interaction) in iFA model and previously published IPF lung tissue. On the
76 right of each heatmap, genes at the extremes of the lists are indicated. At the bottom of each panel, a plot
77 showing running enrichment score (ES) across the ranked list in each pathway is indicated, where the score
78 at the peak of the plot is the final enrichment of the given gene set.

79

80

81

82

83

84

141 **Figure S5. Secondary Screening using the iFA model. Related to Figure 5.**

142 **(A)** Schematic to represent the timeline of prevention and resolution of the iFA phenotype in the iFA

143 model. **(B)** Representative still frames from a time-lapse series showing an invasive and progressive

144 phenotype in the disease model (upper panel), which resolved on addition of AA5 (lower panel); Scale bar,

145 100 μ m. **(C)** Quantitative data presented as mean \pm s.e.m depicting the expression of Collagen I and α -SMA

146 in the iFA model and AA5-presolution cultures collected at day 16. Beta actin was used as a normalization

147 control. n=3, ** $P < 0.01$, * $P < 0.05$ using 2-way ANOVA followed by Sidak's multiple comparisons test.

148 **(D)** Representative IF staining for HMGB1 in DMSO-treated, AA5-prevention- and AA5-resolution-treated

149 iFA model revealing the absence or significantly reduced cytoplasmic HMGB1 in the AA5-treated cultures;

150 Scale bar, 50 μ m. Bottom panels are higher magnification of insets; Scale bar, 25 μ m. **(E)** Overlaid

151 histogram plot that depict the relative SSEA4 fluorescence intensity in the iFA model with DMSO (blue),

152 AA5-prevention (orange) and AA5-reversal (green) treatments. Unstained control is depicted in red. Inset

153 depicts % of positive cells (n=6). ** $P < 0.01$, * $P < 0.05$ using two-tailed paired t-test. The percentage of

154 SSEA4+ cells was significantly reduced in the iFA model with AA5 treatment. **(F-H)** The Rank Rank

155 Hypergeometric Overlap (RRHO) analysis shows statistically significant hypergeometric overlap between

156 differentially expressed genes in the iFA model post AA5-prevention (n=2) and post AA5-resolution (n=2)

157 treatments, as compared to the untreated control, iFA (n=2). This suggests a similar mechanism of action

158 between AA5 in preventing **(G)** and resolving **(H)** fibrosis, and both produce a shift in the gene expression

159 levels that is comparable to the differential expression of genes in the lung IPF tissue (n=7) in contrast to

160 healthy lung controls (n=8), **(G,H)**. The signed, log₁₀-transformed t-test P -values are indicated in the color

161 scale bar. At the bottom and on the left, ranked gene lists are indicated. **(I-J)** The list of significantly

162 enriched terms using ClueGO analysis of AA5-mediated prevention **(I)** and resolution **(J)** of iFA phenotype

163 in the iFA model. Terms are grouped according to the functional group that they belong to. Terms that are

164 part of more than one functional group are shown in purple. The group p-values (corrected with Bonferoni

165 step down) are indicated in between the bar charts. The bars indicate the percentage of the up- (red) or

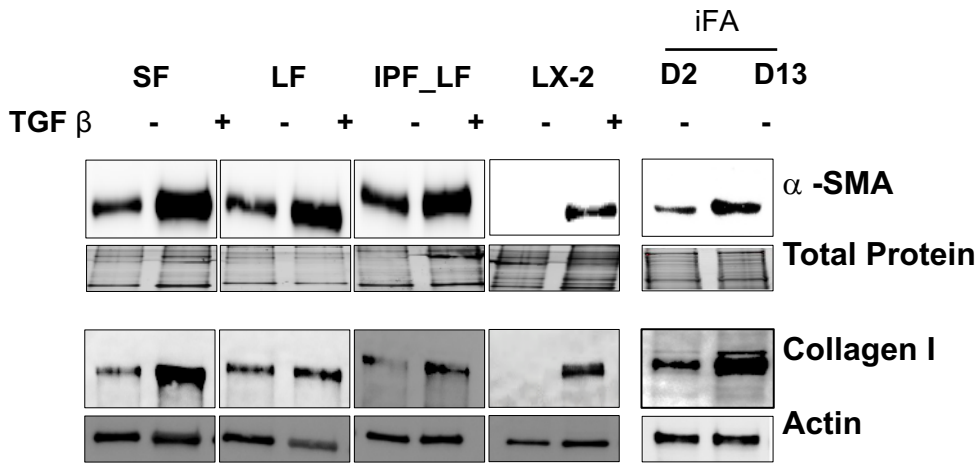
166 down-regulated (blue) genes per each term. The numbers outside the bars show the actual number of genes

167 associated with the specific terms, while the numbers in the parenthesis show the individual term p-value.

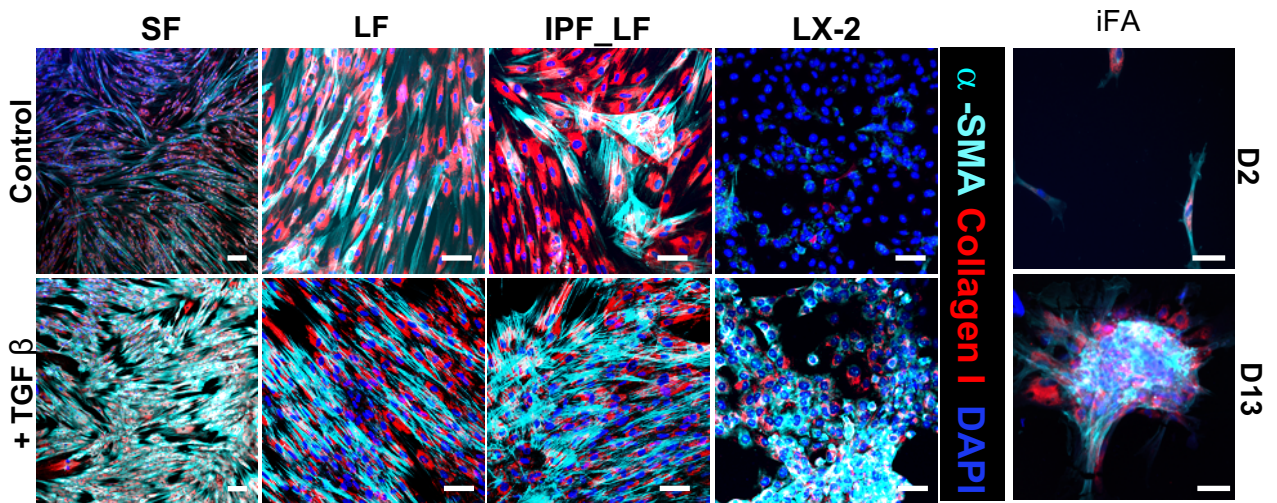
168 Related to Figure 5d-e. **(K)** Representative immunoblot analysis of the expression of p-SMAD2/3 in iFA

FIGURE S3

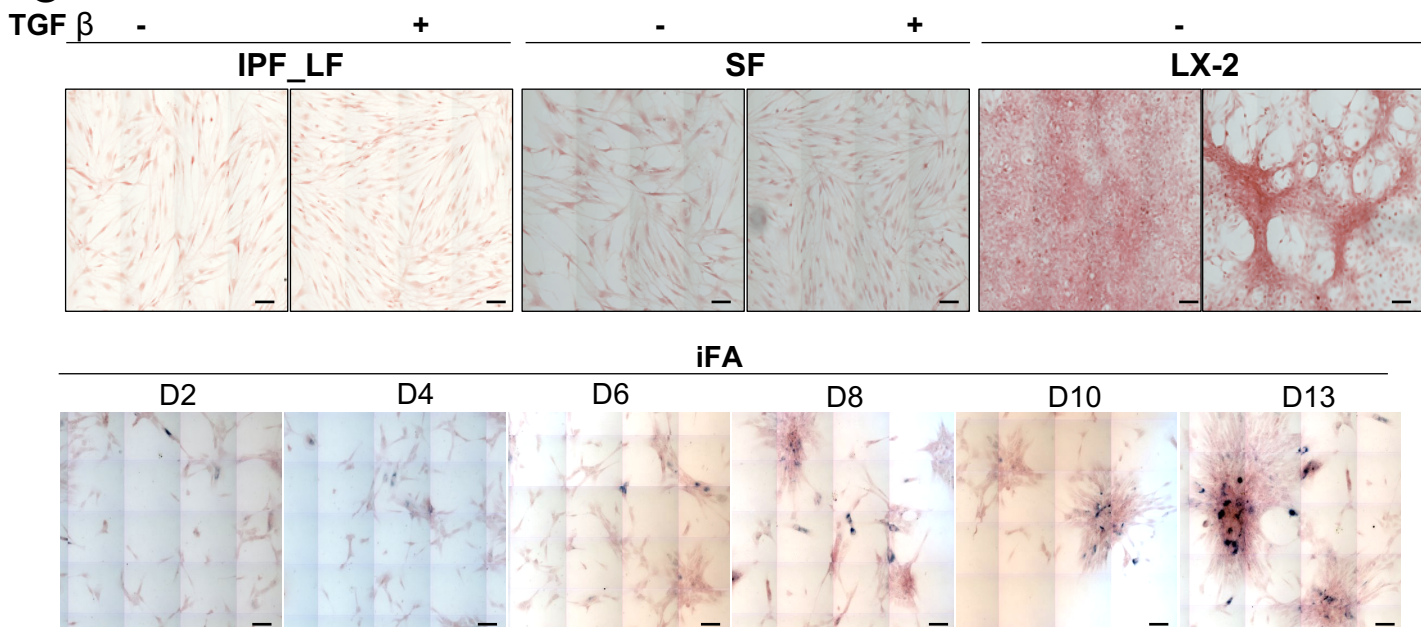
A



B



C



85 **Figure S3. Comparison of iFA Model with TGF- β -Induced Fibrosis Models. Related to Figure 3**

86 **(A)** Representative immunoblot analysis of the expression of Collagen I and α -SMA in exogenously TGF-
87 β -treated fibrosis models of skin (SF), lung (LF, IPF_LF) and liver (LX-2) at 48 hours compared to the iFA
88 model at Day (D) 2 and 13 with no addition of TGF- β . Total protein (α -SMA) and ACTB (Collagen I)
89 were used as a loading controls. **(B)** Representative IF images of Collagen I and α -SMA in exogenously
90 TGF- β -treated fibrosis models of skin (SF), lung (LF, IPF_LF) and liver (LX-2) compared to the iFA
91 model at Day (D) 2 and 13 with no addition of TGF- β . Scale bars, 50 μ m. **(C)** Representative images of
92 exogenously TGF- β -treated fibrosis models of skin, lung and liver (48 hrs) compared to the iFA model
93 during the progression of the fibrotic phenotype the iFA model at day (D) 2 to 13 of culture, demonstrating
94 senescent cells with SA- β -Gal staining; Scale bars, 50 μ m.

95

96

97

98

99

100

101

102

103

104

105

106

107

108

109

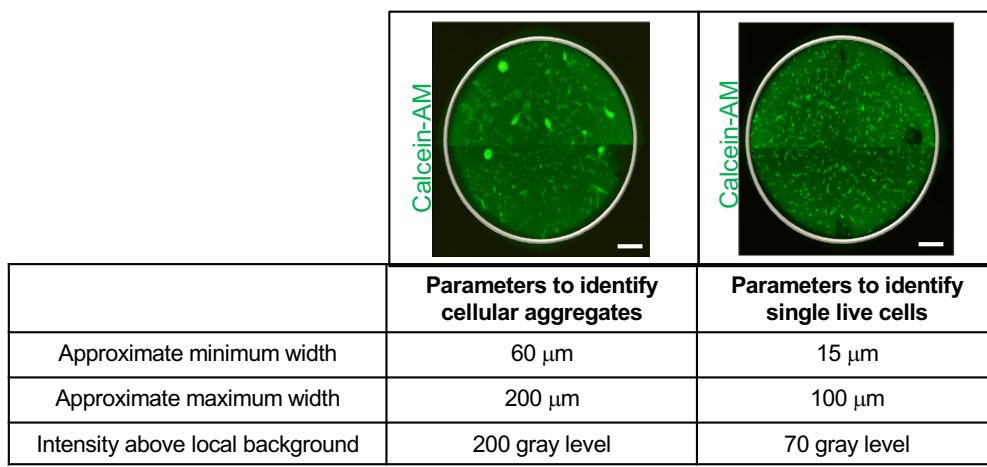
110

111

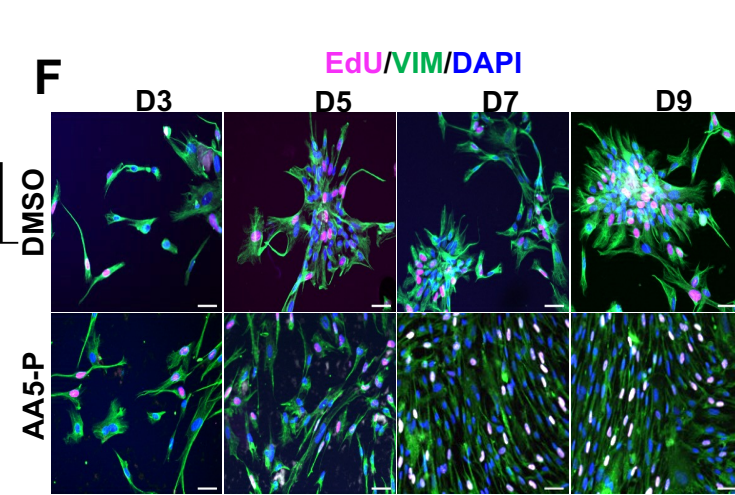
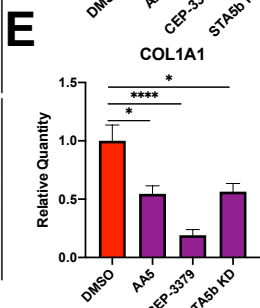
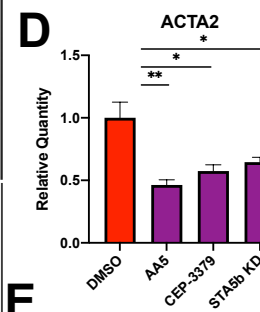
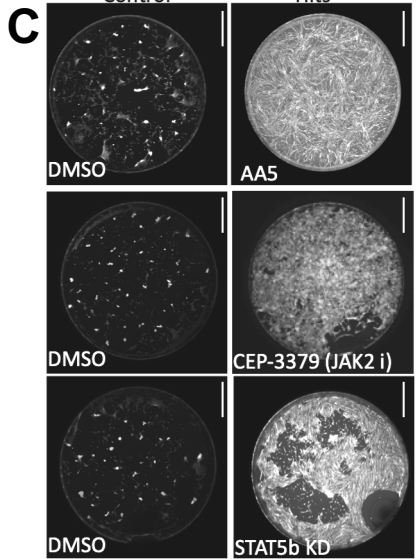
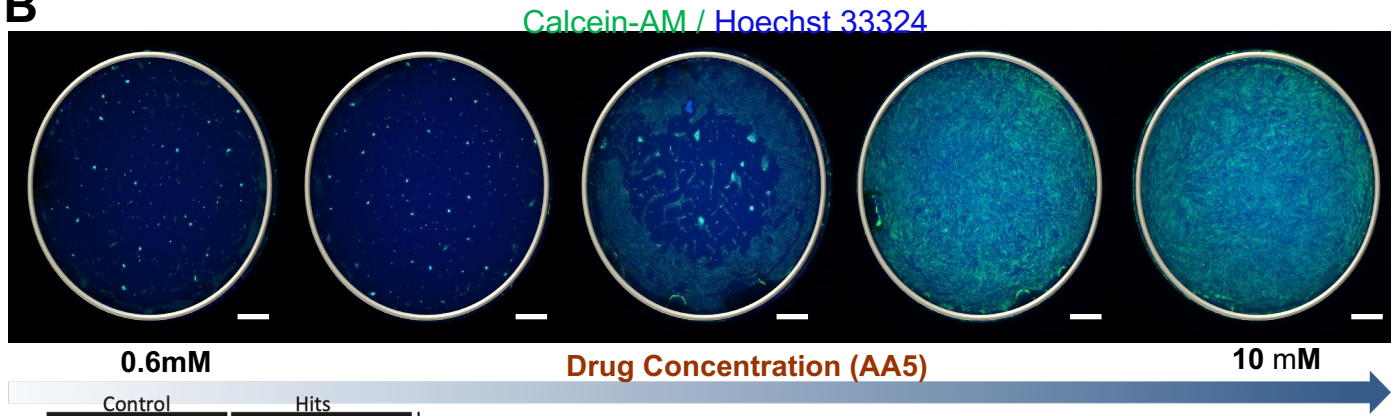
112

FIGURE S4

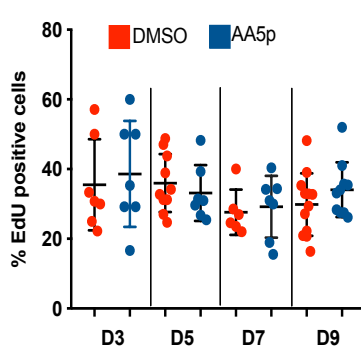
A



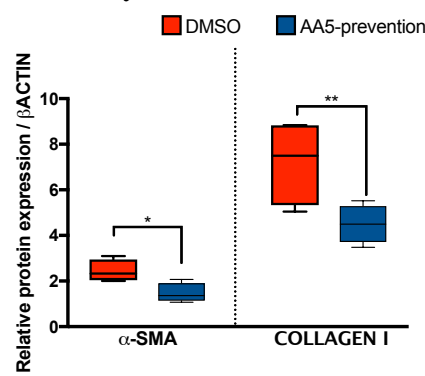
B



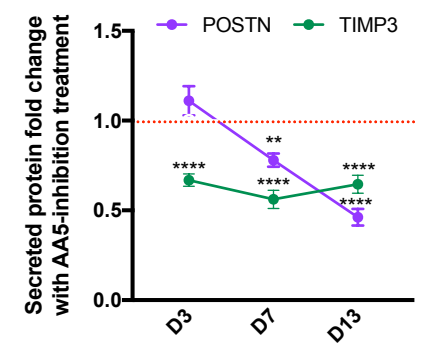
G



H



I



113 **Figure S4. HTS using the iFA model identifies a primary hit molecule. Related to Figure 4.**
114 **(A)** High content staining discrimination of iFA phenotype vs individual spindle-shaped live cells. Cells
115 are stained with Calcein-AM vital dye. Table shows the parameters that were used to identify and count the
116 number of areas displaying the iFA phenotype and total number of individual spindle-shaped live cells.
117 Scale bar, 750 μ m. **(B)** Representative images from wells of the iFA model treated with 0.6 μ M – 10 μ M
118 AA5. Cells were stained with viability dye Calcein AM and the nuclei were counterstained with Hoechst
119 33342. Note full prevention of phenotype at low micromolar concentrations; Scale bar, 750 μ m. **(C)**
120 Representative images from wells of the iFA model treated with DMSO control (left panel), hit molecules
121 (right panel) stained with Calcein AM. No inhibition of the iFA phenotype was observed in the controls.
122 The right panel shows partial or complete inhibition of the iFA phenotype. Scale bar, 750 μ m. **(D-E)**
123 Relative expression of gene expression of *ACTA2* (D) and *COL1A1* (E) in controls, hits and non-hits using
124 the iFA model. **** $P < 0.0001$ * $P < 0.05$ using two-way ANOVA and Sidak's multiple comparison test.
125 **(F)** Comparative IF images of DMSO (top panel) and AA5-prevention (bottom panel) treated iFA model
126 from days (D) 3, 5, 7, and 9 in culture labeled with EdU for 6 hours. The cells were counterstained with
127 VIM and DAPI. Scale bar, 50 μ m. **(G)** EdU positive DAPI cells from (c) was quantified for each time point.
128 Treatment with AA5 did not display any significant difference in the proliferation rate when compared to
129 the DMSO treated cells. All data are presented as the mean \pm s.e.m; non-significant data using one-way
130 ANOVA and Tukey's multiple comparison test. **(H)** Quantitation of immunoblot analysis of the expression
131 of Collagen I and α -SMA in the DMSO and AA5-prevention samples at D8. ACTB was used as a loading
132 control. **(I)** Time-dependent fold change in secreted POSTN and TIMP-3 in response to AA5-prevention
133 treatment versus DMSO in the development of the iFA phenotype (D3 to D13).

134

135

136

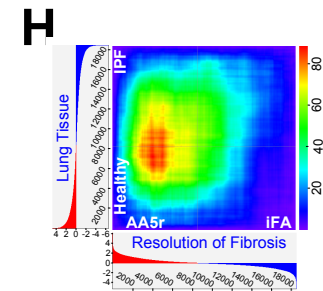
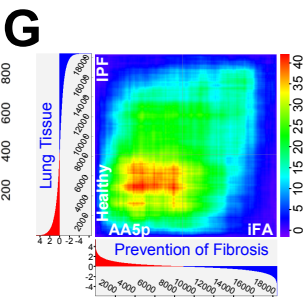
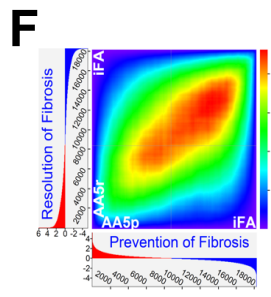
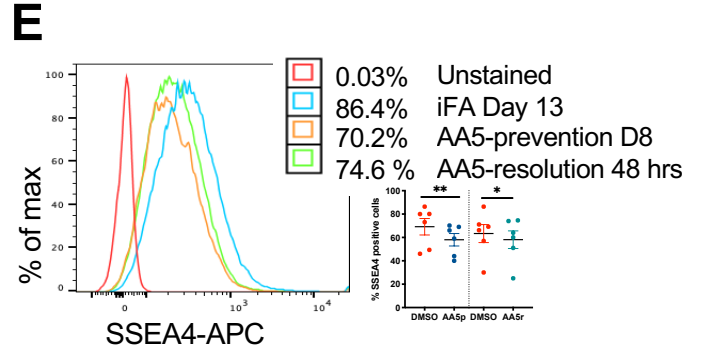
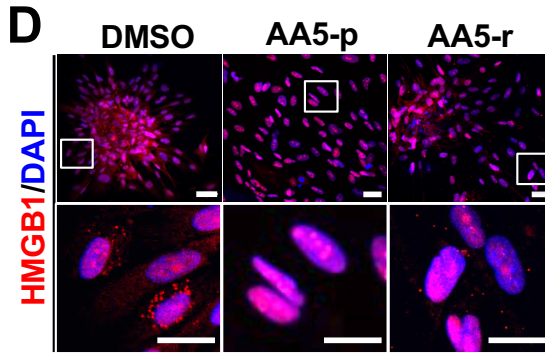
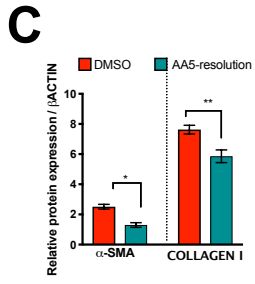
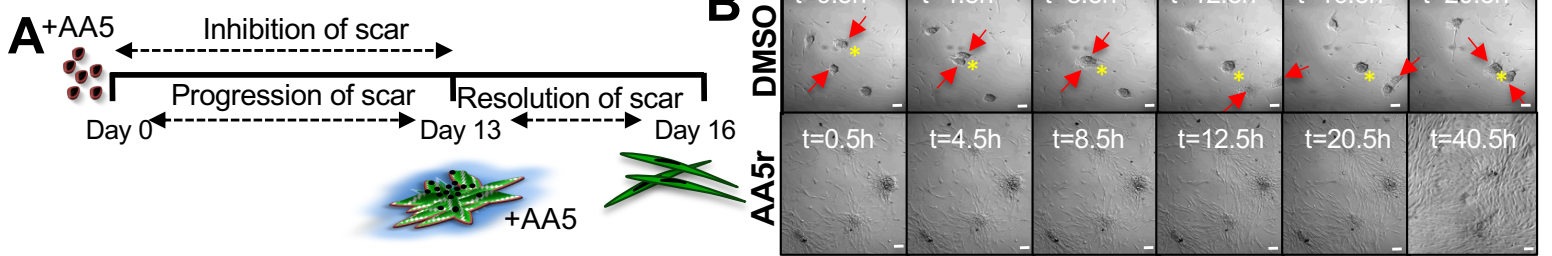
137

138

139

140

FIGURE S5



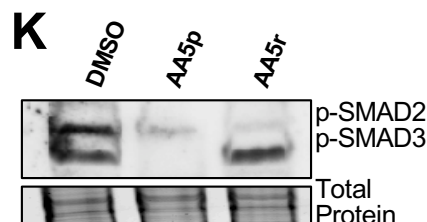
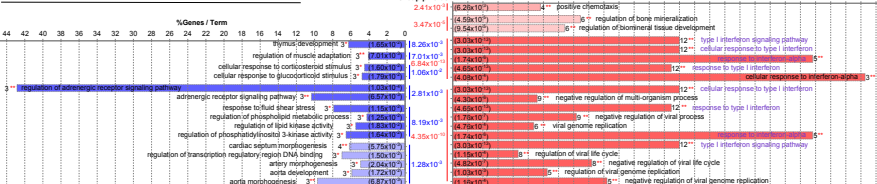
I Prevention of iFA phenotype (DMSO vs AA5 prevention)

Inhibition of Fibrosis: DMSO vs AA5



J Resolution of iFA phenotype (DMSO vs AA5-resolution)

Reversal of Fibrosis: DMSO vs AA5r



141 **Figure S5. Secondary Screening using the iFA model. Related to Figure 5.**

142 **(A)** Schematic to represent the timeline of prevention and resolution of the iFA phenotype in the iFA

143 model. **(B)** Representative still frames from a time-lapse series showing an invasive and progressive

144 phenotype in the disease model (upper panel), which resolved on addition of AA5 (lower panel); Scale bar,

145 100 μ m. **(C)** Quantitative data presented as mean \pm s.e.m depicting the expression of Collagen I and α -SMA

146 in the iFA model and AA5-presolution cultures collected at day 16. Beta actin was used as a normalization

147 control. n=3, ** $P < 0.01$, * $P < 0.05$ using 2-way ANOVA followed by Sidak's multiple comparisons test.

148 **(D)** Representative IF staining for HMGB1 in DMSO-treated, AA5-prevention- and AA5-resolution-treated

149 iFA model revealing the absence or significantly reduced cytoplasmic HMGB1 in the AA5-treated cultures;

150 Scale bar, 50 μ m. Bottom panels are higher magnification of insets; Scale bar, 25 μ m. **(E)** Overlaid

151 histogram plot that depict the relative SSEA4 fluorescence intensity in the iFA model with DMSO (blue),

152 AA5-prevention (orange) and AA5-reversal (green) treatments. Unstained control is depicted in red. Inset

153 depicts % of positive cells (n=6). ** $P < 0.01$, * $P < 0.05$ using two-tailed paired t-test. The percentage of

154 SSEA4+ cells was significantly reduced in the iFA model with AA5 treatment. **(F-H)** The Rank Rank

155 Hypergeometric Overlap (RRHO) analysis shows statistically significant hypergeometric overlap between

156 differentially expressed genes in the iFA model post AA5-prevention (n=2) and post AA5-resolution (n=2)

157 treatments, as compared to the untreated control, iFA (n=2). This suggests a similar mechanism of action

158 between AA5 in preventing **(G)** and resolving **(H)** fibrosis, and both produce a shift in the gene expression

159 levels that is comparable to the differential expression of genes in the lung IPF tissue (n=7) in contrast to

160 healthy lung controls (n=8), **(G,H)**. The signed, \log_{10} -transformed t-test P -values are indicated in the color

161 scale bar. At the bottom and on the left, ranked gene lists are indicated. **(I-J)** The list of significantly

162 enriched terms using ClueGO analysis of AA5-mediated prevention **(I)** and resolution **(J)** of iFA phenotype

163 in the iFA model. Terms are grouped according to the functional group that they belong to. Terms that are

164 part of more than one functional group are shown in purple. The group p-values (corrected with Bonferoni

165 step down) are indicated in between the bar charts. The bars indicate the percentage of the up- (red) or

166 down-regulated (blue) genes per each term. The numbers outside the bars show the actual number of genes

167 associated with the specific terms, while the numbers in the parenthesis show the individual term p-value.

168 Related to Figure 5d-e. **(K)** Representative immunoblot analysis of the expression of p-SMAD2/3 in iFA

169 model treated with either DMSO, AA5-prevention (8 days) or AA5-resolution (48hrs) treatments. Total
170 protein was used as a loading control.

171

172

173

174

175

176

177

178

179

180

181

182

183

184

185

186

187

188

189

190

191

192

193

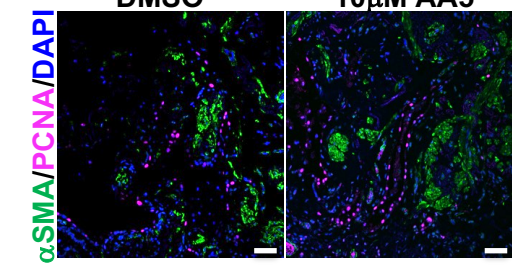
194

195

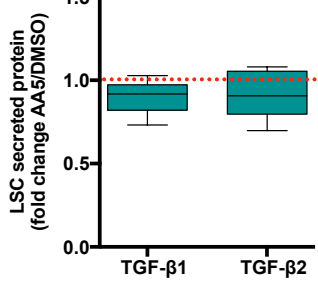
196

FIGURE S6

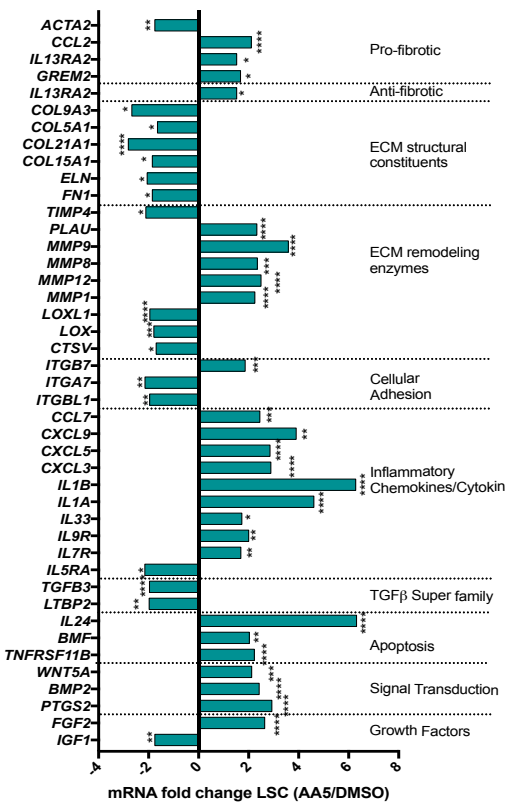
A



B



C



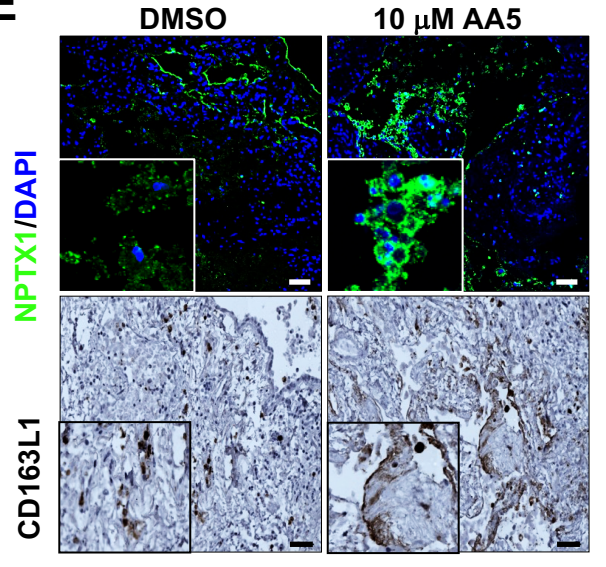
D

Lung Slice Culture: DMSO vs AA5

Group p-value	%Gene Term	%Gene Term
7.65e-11	1	1
3.25e-10	2	2
1.62e-09	3	3
1.75e-10	4	4
8.89e-10	5	5
4.48e-10	6	6
2.26e-10	7	7
1.44e-10	8	8
1.52e-10	9	9
8.51e-10	10	10
1.02e-10	11	11
4.11e-10	12	12
8.15e-10	13	13
5.29e-10	14	14
1.56e-10	15	15
1.61e-10	16	16

- 1: positive regulation of angiogenesis
- 2: positive regulation of cell proliferation
- 3: positive regulation of endothelial cell proliferation
- 4: positive regulation of leukocyte migration
- 5: positive regulation of leukocyte chemotaxis
- 6: positive regulation of leukocyte migration
- 7: positive regulation of leukocyte chemotaxis
- 8: positive regulation of leukocyte migration
- 9: positive regulation of leukocyte chemotaxis
- 10: positive regulation of leukocyte migration
- 11: positive regulation of leukocyte chemotaxis
- 12: positive regulation of leukocyte migration
- 13: positive regulation of leukocyte chemotaxis
- 14: positive regulation of leukocyte migration
- 15: positive regulation of leukocyte chemotaxis
- 16: positive regulation of leukocyte migration

E



197 **Figure S6. *Ex vivo* anti-fibrotic effect of AA5. Related to Figure 6**

198 **(A)** Representative image of DMSO- and AA5-treated lung slice cultures (LSCs) stained for the
199 proliferation marker PCNA 72 hours after treatment depicting viability of tissue. Samples were
200 counterstained for α -SMA and DAPI. **(B)** Relative secreted levels of TGF- β proteins in supernatants of
201 AA5-treated LSCs compared to DMSO-treated controls, 48 hours after treatment (n=9). Data represent
202 min-max and median protein abundance in AA5-treated LSCs relative to DMSO treated controls (red line).
203 **(C)** Gene expression analysis showing relative expression levels of fibrosis-related genes in LSCs treated
204 with AA5 compared with DMSO treatment depicting the fibro-protective effect of AA5 (n=6). TMM
205 (trimmed mean of M-values) was used to normalize the gene expression; **** $P < 0.0001$ *** $P < 0.001$ **
206 $P < 0.01$ * $P < 0.05$. **(D)** The list of significantly enriched terms in the ClueGO analysis from the pairwise
207 comparison between AA5 and DMSO treated LSCs. Terms are grouped according to the functional group
208 that they belong to. Terms that are part of more than one functional group are shown in purple. The group
209 p-values (corrected with Bonferoni step down) are indicated in between the bar charts. The bars indicate the
210 percentage of the up- (red) or down-regulated (blue) genes per each term. The numbers outside the bars
211 show the actual number of genes associated with the specific terms, while the numbers in the parenthesis
212 show the individual term p-value. **(E)** Upper panel shows representative images of DMSO- and AA5
213 (10 μ M)-treated LSCs stained for NPTX1 revealing excessive NPTX1 staining in the honey comb cyst areas
214 of the IPF lung in the AA5-treated samples within 48 hours of treatment in comparison to the DMSO
215 controls. The samples were counterstained for DAPI. Insets are higher magnified images. Scale bar, 50 μ m.
216 Lower panel shows representative images of DMSO- and AA5 (10 μ M)-treated LSCs stained for scavenger
217 receptor protein CD163L1 by immunohistochemistry and revealed prominent staining on macrophages in
218 both treatments, but a higher expression of shed receptor staining was seen on AA5 treatment suggesting
219 activation of the phagocytic cells. Insets are higher magnified images. Scale bar, 100 μ m.

220

221

222

223

224

A

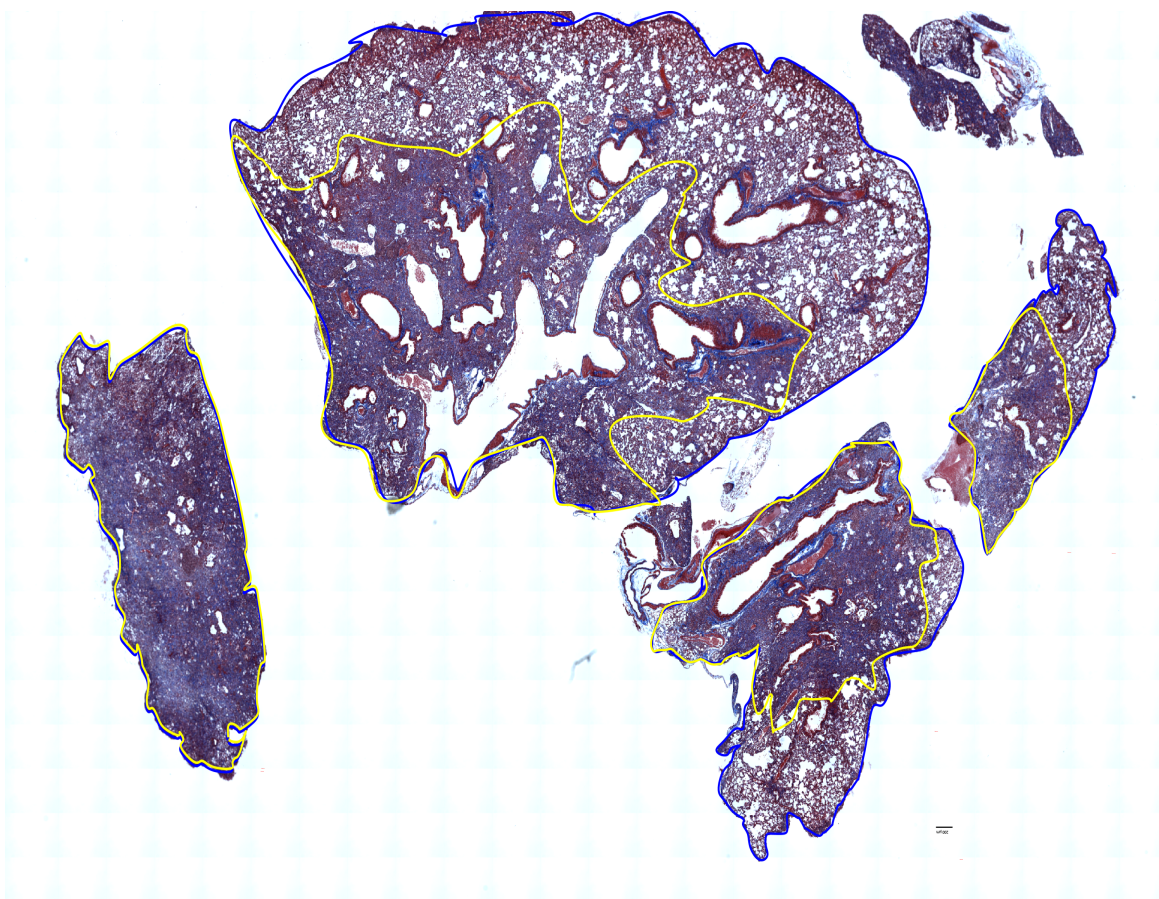


Figure S7. *In vivo* anti-fibrotic effect of AA5. Related to Figure 7.

(A) Representative Masson trichrome stained section of bleomycin treated lungs with the borders of the lung and fibrotic areas marked using the spline contour tool. Percent fibrotic area was calculated for each lobe (related to Figure 7J) Scale bars, 100 μm .

S.No	Patients	Tissue source	Age	Gender
1	IPF patient 1	Lung, skin	65	F
2	IPF patient 2	Lung, skin	55	M
3	IPF patient 3	Lung, skin	62	M
4	IPF patient 4	Lung, skin	50	F
5	IPF patient 5	Lung, skin	64	M
6	No prior disease patient 1	lung	NK	NK
7	No prior disease patient 2	lung	NK	NK
8	No prior disease patient 3	lung	NK	NK
9	No prior disease patient 4	lung	NK	NK
10	No prior disease patient 5	lung	NK	NK
11	No prior disease patient 6	lung	NK	NK
12	No prior disease patient 7	blood	NK	M
13	No prior disease patient 8	skin	NK	M
14	No prior disease patient 9	skin	NK	M
15	Patient with NKx2.1 mutation #1	skin	NK	M
16	Patient with NKx2.1 mutation #2	Skin	NK	F
17	Patient with NKx2.1 mutation #3	Skin	NK	F

NK – not known

Table S1: Information of subjects from whom samples were collected for iPSC derivation. Related to Figures 1 and S1.

Oligonucleotides		
<i>TGFB3</i>	Thermo Fisher Scientific	Hs01086000_m1
<i>TIMP1</i>	Thermo Fisher Scientific	Hs01092512_g1
<i>MMP3</i>	Thermo Fisher Scientific	Hs00968305_m1
<i>PLAT</i>	Thermo Fisher Scientific	Hs00263492_m1
<i>LOX</i>	Thermo Fisher Scientific	Hs00942480_m1
<i>PTX3</i>	Thermo Fisher Scientific	Hs00173615_m1
<i>NPTX1</i>	Thermo Fisher Scientific	<i>Hs00982601_m1</i>
<i>CD163L1</i>	Thermo Fisher Scientific	<i>Hs00264549_m1</i>
<i>ACTA2</i>	Thermo Fisher Scientific	Hs00426835_g1
<i>COL1A2</i>	Thermo Fisher Scientific	Hs01028956_m1
<i>TGFB1</i>	Thermo Fisher Scientific	Hs00998133_m1

Table S3: List of TaqMan probes used in this study. Related to Methods.

253 **Table S2:** Canonical pathway enrichment analysis of iFA model compared to previously published fibrotic
254 lung, liver and kidney tissues. Related to Figures 2H and S2E.

255

256

257 **Supplemental Videos:**

258 **Video S1. Time-lapse movie showing pre-iFA phenotype in the model. Related to Figure 1.**

259 Transmitted light time-lapse images of iFA model at Day 4 revealing the initial stages of the formation of
260 the iFA phenotype. The time-lapse covers a period of about 17 hours, imaged every 8 minutes and exported
261 at 12 frames per second.

262

263 **Video S2. Time-lapse movie showing iFA phenotype in the model. Related to Figures 1 and S5B.**

264 Transmitted light time-lapse images of iFA model at Day 13 revealing fully established iFA phenotype at
265 Day 13. The time-lapse covers a period of about 20 hours, imaged every 8 minutes and exported at 12
266 frames per second. The clusters show directionality, likely a consequence of the chemokine/cytokine
267 secretion, combing of clusters accounting for the progressively increasing size of the clusters.

268

269 **Video S3. Time-lapse movie showing the iFA-resolution effect of AA5. Related to Figures 5 and S5B.**

270 Transmitted light time-lapse images of iFA model at Day 13, 5 hours after addition of 10 μ M AA5 revealing
271 full resolution of the iFA phenotype within 48 hours. The time-lapse covers a period of about 20 hours,
272 imaged every 8 minutes and exported at 12 frames per second.

273

274

275

276

277

278

279